PHYSICAL
ACOUSTICS

Acousto-Optic Interaction in Laser Vibrometry in a Liquid

O. A. Sapozhnikov[a], A. V. Morozov[a], and D. Cathignol[b]

[a] *Physics Faculty, Moscow State University, Moscow, 119991 Russia*
e-mail: oleg@acs366.phys.msu.ru
[b] *INSERM Unité 556, 151 Cours Albert Thomas, 69008 Lyon, France*
Received October 19, 2008

Abstract—It is demonstrated that, when the classical method of laser vibrometry is used for measurements in a liquid, it gives erroneous results with measurement errors reaching 100% or more. The vibration pattern observed in this case exhibits a false structure with a spatial scale identical to the wavelength of acoustic waves in the liquid. In addition, the laser vibrometer shows displacements in the regions where they are actually absent. In the transient mode of operation, the image displays nonexistent surface waves, which propagate with the velocity of sound in the liquid. The origin of these distortions lies in the acousto-optic interaction that occurs in the condensed medium on the path of the probing laser beam. An analytic expression is obtained for the Green's function characterizing laser vibrometry in the cases of harmonic and pulsed excitation of the surface under investigation. It is shown that this function explains all the artifacts observed in laser vibrometry in a liquid and can be used to correct the measurement data.

1. INTRODUCTION

Laser vibrometry is one of the methods for measuring displacements of light-reflecting surfaces [1]. The method is based on measuring the phase shift of a light wave due to its reflection from a given point on the surface. It provides high resolution in both space (usually, about 0.1 mm) and time (up to 10^{-8} s). At the same time, the measuring laser can be positioned at a relatively large distance from the object under investigation. Owing to these advantages, laser vibrometers are widely used in various fields of science and engineering. In particular, this method can be used for studying the operation of ultrasonic transducers [2, 3].

When using laser vibrometers, one should take into account that they are intended for measurements under the condition that the displacement of the surface under investigation is the only reason for the phase variation in the probing laser beam. This is true when the path of the laser beam does not intersect any nonstationary inhomogeneities of the refraction index, which cause additional uncontrolled phase shifts. If the measurements are performed in vacuum or in a homogeneous gas, the aforementioned condition is satisfied. In transparent liquids and solids, the situation is different: surface vibrations cause variations in the density of the medium, which can make the method inapplicable. In some publications, this fact was ignored and, therefore, conclusions concerning the type of surface vibrations of interest were erroneous. In the present paper, we study the signal of a laser vibrometer in the case when the vibrating surface under test is placed in a condensed medium.

2. EXPERIMENTAL DEMONSTRATION OF THE EFFECT OF ACOUSTO-OPTIC INTERACTION

Experiments demonstrating the significance of the effect of acousto-optic interaction on the operation of a laser vibrometer were carried out under the joint research program by the Department of Acoustics of the Physics Faculty of Moscow State University and the Laboratory of Acoustics of the National Institute of Health and Medical Research, France (INSERM, Unité 556). The experimental setup is shown in Fig. 1. The piezoelectric transducer under investigation was placed in a tank filled with a transparent liquid. One of the walls of the tank had a transparent window made from a plane-parallel fused silica plate. Through this window, the probing beam of the laser vibrometer was transmitted to the transducer. A plastic membrane with a gold layer deposited on it was positioned parallel to the radiating surface at a distance of 0.5 mm from it. The membrane was very thin (10 μm) and therefore presented no obstacle for ultrasound propagation. At the same time, the membrane efficiently reflected the probing laser beam. Since the distance from the membrane to the transducer was much smaller than the wavelength of ultrasound, the displacement of its surface differed little from the surface displacement of the piezoelectric plate. In the course of measurements, the membrane remained fixed while the transducer moved parallel to it with the help of a computer-controlled positioning system. To reduce undesired vibration, the tank and the laser vibrometer were mounted on an optical bench. The laser vibrometer used in the
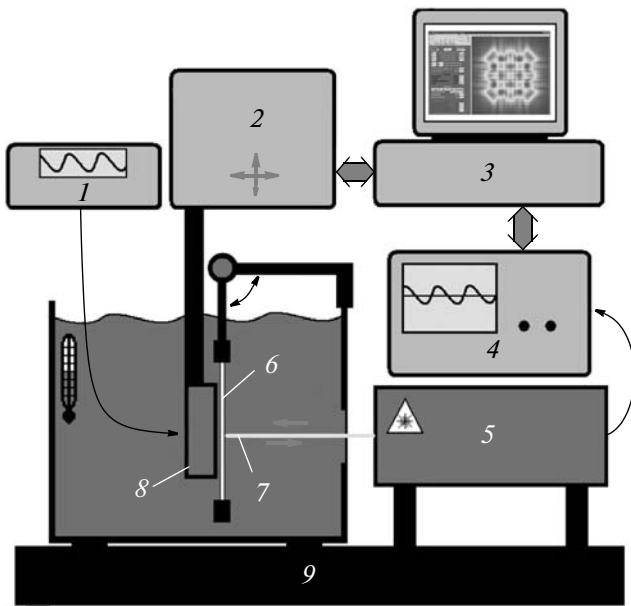
SAPOZHNIKOV et al.

Fig. 1. Measuring setup for laser vibrometry in a liquid: (*1*) oscillator, (*2*) positioning device, (*3*) computer, (*4*) oscilloscope, (*5*) laser vibrometer, (*6*) light-reflecting membrane, (*7*) probing laser beam, (*8*) transducer under investigation, and (*9*) optical bench.

experiments was a commercial instrument of The Thales Laser S.A. SH-140 type (made in France), which could measure displacements with amplitudes of up to 100 Å. The analog output signals of the laser vibrometer were supplied to a digital oscilloscope and, via a GPIB interface, to a computer for processing. In the case of measurements in air, the reflecting membrane was attached to the surface of the transducer, all other parameters of the setup were the same.

The setup described above was used to study surface vibrations of various transducers. Here, we consider only one of them: a square transducer with the dimensions 4 × 4 cm, which had a thickness resonance fre-

quency of 1 MHz. The transducer was made from 1−3 piezocomposite material. The 1−3 piezocomposite consists of a set of small-size piezoceramic columns embedded in a polymer material of epoxy resin [4]. In contrast to piezoceramics, piezocomposite provides a strong suppression of Lamb waves [5, 6].

Figure 2 shows the results of measuring the displacements of the transducer surface in a continuous mode of operation at a frequency of 1 MHz. The left-hand image represents the distribution of the displacement amplitude obtained from measurements in air, and the right-hand image is obtained from measurements in water. The central image is the X-ray image of the transducer structure. The fine structure of the piezocomposite is visible in X-rays, but does not manifest itself in the distribution of the displacement amplitude measured by the vibrometer. However, coarser inhomogeneities are rather clearly defined. Note that the structure of the piezocomposite is deliberately made aperiodic with the aim to avoid undesirable resonance phenomena. The aperiodicity is seen in both the X-ray image and the image obtained from laser vibrometry in air. In the case of measurements in water, the visible inhomogeneity of velocity proved to be strictly periodic with the step of this structure being 1.5 mm, which exactly coincides with the wavelength of ultrasound in water. As it will be seen below, because of the acousto-optic interaction, a strong "grid" with a spatial period identical to the acoustic wavelength in the liquid is superimposed on the true distribution of the displacement amplitude and masks this distribution. The nature of the grid will be explained below.

The effect of acousto-optic interaction is even more pronounced in the pulsed mode of excitation, when a short exciting pulse is supplied to the transducer. In this case, regions of structure inhomogeneities of the piezoelectric plate may become sources of surface waves. Since the experiments were performed with a piezocomposite, these waves should be strongly suppressed. Measurements were carried out in air and in two liquids: water and glycerol. Additional measure-
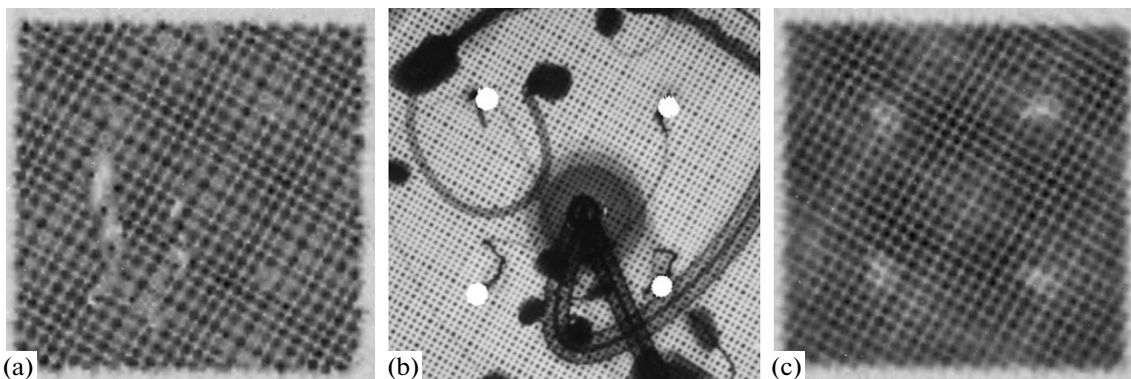

Fig. 2. (a) Distribution of the amplitude of surface displacement for a piezocomposite transducer in the continuous mode of excitation in air. The scan step is 0.5 mm; the darker regions correspond to higher amplitudes of displacement (a linear grey scale is used). (c) A similar distribution measured in water. (b) An X-ray image of the transducer structure on the same scale.
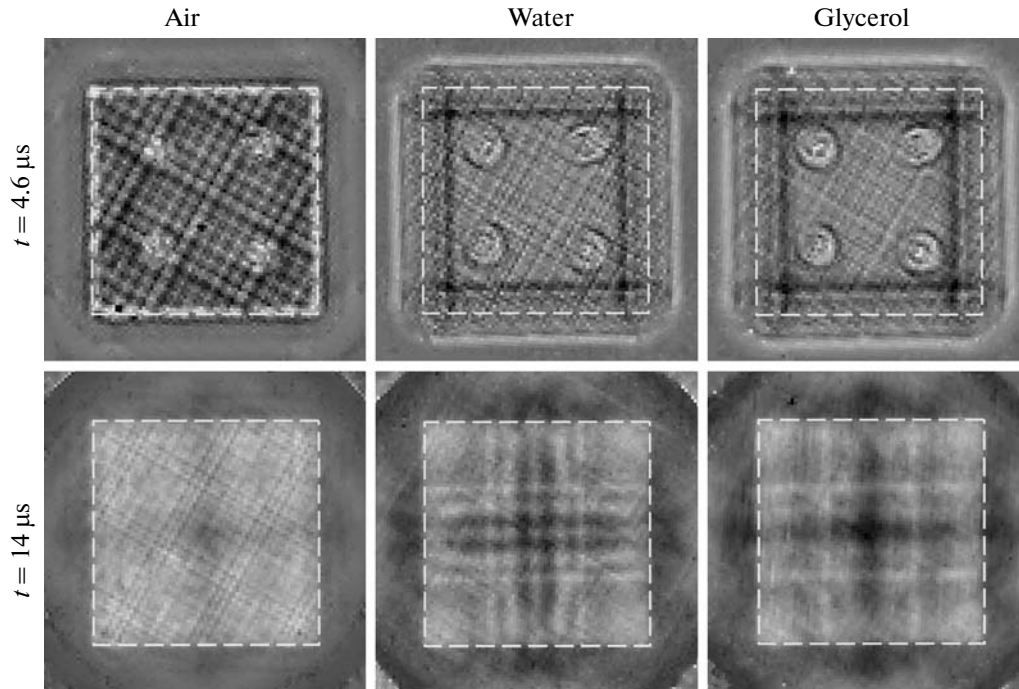
Fig. 3. Distribution of the displacement of the transducer surface measured in the pulsed mode of excitation. The boundary of the transducer is indicated by the white dashed line. The scan step is 0.6 mm. The measurements were performed in air, in water, and in glycerol. The type of the medium is indicated at the top, and the instant of measurement at the left.

ments with glycerol, in which the velocity of sound is widely different from that in water (1.9 mm/μs and 1.5 mm/μs, respectively) allowed us to verify the assumption that precisely the acousto-optic interaction is responsible for the appearance of artifacts in laser vibrometry. Typical results are shown in Fig. 3.

The measurements in air revealed the presence of surface waves. They were clearly visible at the initial instants of time as diverging circles near the four points of electric contacts (the upper left image). These waves rapidly decayed. In addition, weak disturbances traveling from the edges and converging at the center of the transducer could be noticed. These disturbances were almost invisible at the initial instants of time and manifested themselves only when they converged at the center of the transducer by forming a characteristic cross (the lower left image). The velocity of waves could be determined from the time of the cross formation and was found to be about 2 mm/μs. When the transducer was placed in a liquid, these waves became leaky waves, and therefore they could be expected to attenuate. Indeed, they were not noticeable in the experiments with water and glycerol. However, unlike the case of observations in air, the images obtained from laser vibrometry in liquids showed strong disturbances propagating over the surface from the points of contacts and from the edges (the central and right-hand columns of Fig. 3). As will be shown below, these disturbances are artifacts caused by acousto-optic interaction. The pattern obtained in this case from the

laser vibrometer is the shadow image of edge waves, which has no direct relationship to the true surface displacement. The aforementioned waves propagate in the liquid rather than in the piezoelectric plate. This is confirmed by the fact that the measured velocity of the displacement of dark strips in the images was different for water and for glycerol. The difference in velocities can be seen in the central and right-hand images of the lower row. One can see that, by the instant $t = 14$ μs, in the case of measurement in water, the "surface waves" propagating from the edges did not yet converge at the center of the transducer, whereas, in the case of glycerol, they already reached the center and formed the characteristic cross. The measured velocity of the front of these disturbances coincided with the velocity of sound in the corresponding liquids: 1.5 mm/μs in water and 1.9 mm/μs in glycerol.

Thus, when displacements of the surface placed in a liquid are measured with the use of laser interferometry, strong false signals appear which have no direct relationship to the true displacements. We note that, at certain instants of time, the amplitude of these false signals exceeds the true displacement; i.e., acousto-optic interaction is an important factor that cannot be ignored.

3. THEORETICAL ANALYSIS OF THE SIGNAL OF A LASER VIBROMETER WITH ALLOWANCE FOR ACOUSTO-OPTIC INTERACTION

3.1. Calculation of the Optic Phase Incursion

We consider a plane acoustic transducer whose surface is at $z = 0$. In the course of vibrations, the surface is displaced and acquires the coordinate $z = \xi(x,y,t)$, where the displacement ξ is a function of transverse coordinates x, y and time t. The beam of the probing light from a laser is incident on the aforementioned surface in the direction perpendicular to it, is reflected from the surface and propagates in the backward direction. Then, the light beam arrives at the interferometer, where the phase shift between the incident and reflected light waves is measured. Since the light beam travels the distance between the source and the surface twice, it acquires the following phase shift:

$$\varphi = (4\pi/\lambda) \int_\xi^L n(\mathbf{r},t)dz, \tag{1}$$

where λ is the wavelength of the light wave in vacuum; L is the thickness of the layer of the medium lying on the path between the vibrometer and the surface; and n is the refractive index, which depends on the coordinates and on time in general. Even when the medium in the initial state is optically homogeneous, its homogeneity will be violated because of the acoustic wave emitted into it by the vibrating surface. In this case, $n(\mathbf{r},t) = n_0 + \gamma p(\mathbf{r},t)$, where n_0 is the unperturbed refractive index, $\gamma = dn/dp$ is the acousto-optic coefficient and $p(\mathbf{r},t)$ is the sound pressure. In general, the refractive index is determined by the density of the medium [7], but, in the acoustic wave, the density variation is proportional to the sound pressure.

The inhomogeneity of the refraction index may cause not only an additional phase shift, but also a refraction of the beam, i.e., its deviation from the initial rectilinear propagation path. As a result of this refraction, the beam will be reflected from a point different from that at which it was initially directed. In addition, a wide deviation of the reflected beam may cause a reduction or even a complete suppression of the laser vibrometer's signal, because the probing and the reference beams will be separated in space and as a consequence, will not interfere with each other. However, the aforementioned refraction of the beam can be insignificant in the case of a weak inhomogeneity of the refraction index, i.e., in the case of small-amplitude vibrations of the transducer surface. Below, we consider this kind of regime. Neglecting the second-order-smallness terms, we represent Eq. (1) in the form [8]

$$\varphi \approx (4\pi/\lambda)\left[n_0(L-\xi) + \gamma \int_0^L p(\mathbf{r},t)dz\right]. \tag{2}$$

One can see that the quantity φ depends not only on the surface displacement at the point of incidence of the laser beam (ξ), but also on the distribution of sound pressure over the entire optic path. In vacuum and in gases, the acousto-optic effect is absent or negligibly small ($\gamma \to 0$); i.e., the phase variation proves to be proportional to the surface displacement: $\Delta\varphi = -(4\pi n_0/\lambda)\xi$, which yields

$$\xi = \Delta\varphi[-\lambda/(4\pi n_0)]. \tag{3}$$

The latter expression is the basic one for laser vibrometry in vacuum and in gases. As it was mentioned above, in condensed media the relationship is not as simple and the neglect of acousto-optic interaction may lead to large errors.

Figure 4 shows an example of a numerical simulation illustrating the role of the acousto-optic effect [9]. The source of ultrasonic radiation was assumed to be a transducer that had the dimensions 4×4 cm and operated at a frequency of 1 MHz in water. The distribution of the component of the normal velocity over the transducer surface was chosen to be nonuniform, which is typical of piezoceramic ultrasonic transducers. Figure 4a shows the distribution of the two-dimensional amplitude of the acoustic field formed in water. The field was calculated using the Rayleigh integral. The sound beam is strongly inhomogeneous, especially near the transducer, and experiences diffraction divergence in the course of its propagation. From Eq. (2), we calculate the phase incursion for the light wave with allowance for the acousto-optic interaction in water. Then, from Eq. (3), we determine the displacement seeming of the surface by neglecting the effect of the medium on the phase of the light wave ($n_0 = 1$, $\gamma = 0$). The resulting velocity distribution corresponding to the data of the laser vibrometer is shown in the lower part of Fig. 4. One can see that the distribution of the seeming velocity widely differs from the true one. In particular, the velocity structure acquires additional vibrations with a spatial period approximately identical to the ultrasonic wavelength in water (1.5 mm). In addition, the seeming transverse size of the transducer is much greater than the actual size: the vibrometer predicts displacements in the region where they are actually absent.

In one important specific case, consideration of acousto-optic interaction is rather simple. Let the surface under study be an infinite plane and let it vibrate as a single unit, i.e., the displacement distribution over the surface be uniform: $\xi = \xi(t)$. In this case, the acoustic wave is a plane wave with $p(\mathbf{r},t) = \rho c\dot{\xi}(t - z/c)$, where ρ

(a)

z

x

V/V_0 (b)

1

0

−20 −10 0 10 20

$\tilde{V}/V_0$ (c)

1

0
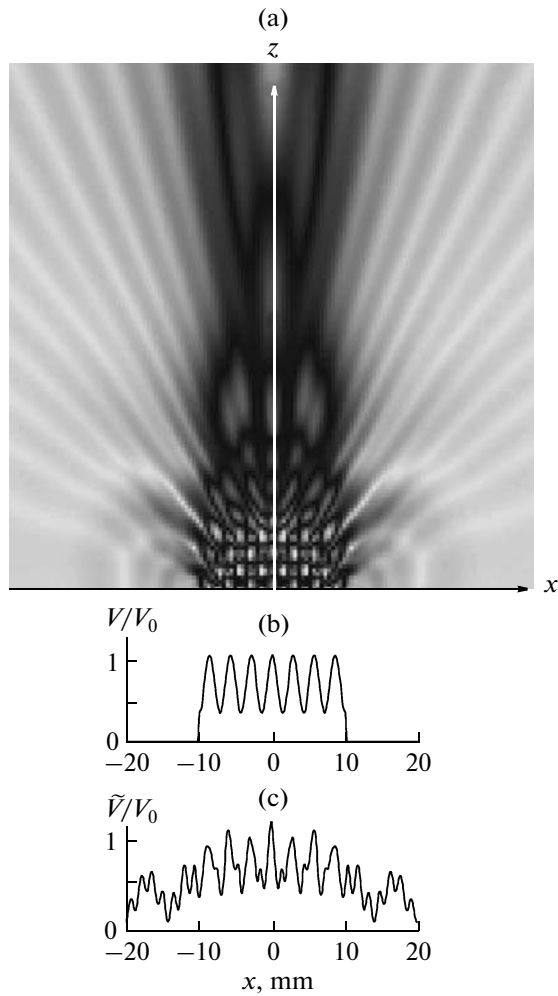
−20 −10 0 10 20

x, mm

Fig. 4. Effect of acousto-optic interaction in the liquid on the data of the laser vibrometer (the results of simulation). (a) Two-dimensional distribution of the amplitude of sound pressure in the xz plane: calculation with the use of the Rayleigh integral. (b) Surface velocity distribution used in simulation (V is the amplitude of the normal velocity component and V_0 is its characteristic value). (c) Data of the laser vibrometer for the velocity amplitude $\tilde{V}$: prediction according to Eq. (3).
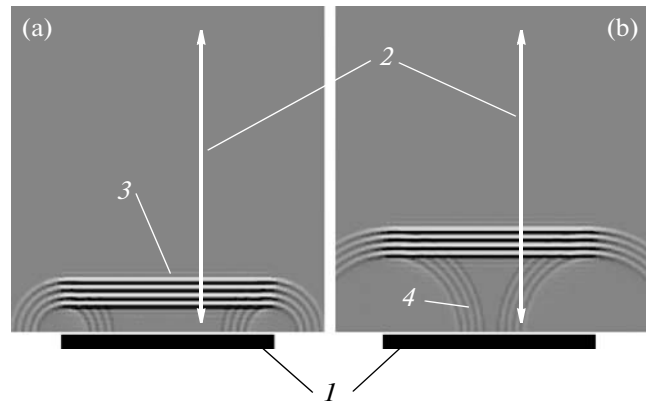

(a)

2

3

(b)

4

1

Fig. 5. Two-dimensional distribution of sound pressure at two sequential instants of time. (*1*) The piston-type source generates a short pulse. (a) Until a certain instant, (*2*) the probing laser beam only intersects (*3*) the direct wave; i.e., the surface displacement can be measured using the plane wave theory. (b) From the instant (*4*) the edge wave reaches the laser beam, the data of the laser vibrometer are distorted by acousto-optic interaction.

and c are the density of the medium and the velocity of sound in it and $\dot{\xi} = d\xi/dt$. We assume that, at the end of the layer of the medium ($z = L$), the acoustic wave is absent because of absorption or because it did not reach the end of the layer by the instant of measurement. Then, from Eq. (2), we obtain $\Delta\varphi = -\left(4\pi n_*/\lambda\right)\xi$, where $n_* = n_0 - \gamma\rho c^2$ has the meaning of the effective refractive index. In condensed media, it widely differs from n_0. For example, in water $n_0 = 1.33$ and $n_* = 1.033$ [10, 11]. The approximation of the plane wave is used, e.g., in calibration of hydrophones by laser vibrometry [10, 12]. In this method, the local sound pressure p is calculated on the basis of measuring the corresponding displacement ξ of a thin light-reflecting membrane. The membrane is positioned in the far-field zone of the source of ultrasound, where the wave can be considered as a plane wave with fair accuracy; i.e., it is possible to use the expression $\Delta\varphi = -\left(4\pi n_*/\lambda\right)\xi$ and then calculate the pressure from the formula $p = \rho c\dot{\xi}$. In the near-field zone, such an approach is inapplicable in the general case: both of the above formulas fail because of the diffraction effects near the transducer. The fact was already discussed above (see Fig. 4). However, when using piezoelectric transducers, in some cases it is possible to apply the approximation of the plane wave in the near field as well, if the measurements are performed in the pulsed mode of operation and a suitable time window is chosen. Indeed, in the case of vibration of a homogeneous plate, the emitted acoustic signal can be represented as a superposition of a "direct" plane wave, and "edge" wave, and a "side" wave generated by Lamb waves. If a transient mode of operation takes place, within a few moments after the beginning of radiation, a spatial region is formed where the direct wave is separated from the edge and side waves.

The corresponding structure of the acoustic field is shown in the left-hand plot of Fig. 5. One can see that the beam of the probing laser directed at the central region of the plate only intersects the direct signal; i.e., the incursion of the optic phase is produced by the plane wave by itself. In the corresponding interval of time, the relations $\Delta\varphi = -\left(4\pi n_*/\lambda\right)\xi$ and $p = \rho c\dot{\xi}$ are satisfied, and, therefore, an absolute pressure measurement can be carried out. Starting from a certain instant, the side wave intersects the laser beam, and then the edge wave arrives (see the right-hand plot of Fig. 5). From this instant on, the regime of the plane

wave is violated. If the distance from the point of measurement to the edge of the transducer is x_* and the maximal velocity of elastic waves in the piezoelectric material is c_*, the duration of the regime of the plane wave is $t_* = x_*/c_*$. Evidently, the plane wave will be emitted only when the characteristics of the piezoelectric plate are homogeneous. This is possible if pore-free piezoceramics or a piezoelectric single crystal is used. If the structure of the piezoelectric material is inhomogeneous (e.g., if a piezocomposite is used), the regime of the plane wave will be impossible.

3.2. Spatial Filtering Caused by Acousto-Optic Interaction (the Direct Problem)

According to Eq. (2), the additional phase incursion of the light wave is proportional to the integral $\int_0^L p(\mathbf{r}, t)dz$; i.e., it is necessary to know the sound pressure at every point of the laser beam. We assume that the liquid is an ideal linear medium; i.e., the effects of viscosity, thermal conduction and acoustic nonlinearity do not manifest themselves. Then, to determine the sound pressure, we have to solve the wave equation $\Delta p - c^{-2}\partial^2 p/\partial t^2 = 0$ with the boundary condition corresponding to a given dependence $\xi(t)$. For the sake of convenience, we change all of the functions of time $f(t)$ to their spectra $F(\omega) = \int_{-\infty}^{+\infty} f(t)e^{i\omega t}dt$. For the spectra of sound pressure $p(x,y,z,t)$, true displacement $\xi(x,y,t)$ and seeming displacement $\hat{\xi}(x,y,t) = n_0\xi - \gamma\int_0^L p(\mathbf{r}, t)\,dz$, we use the notations $P(x,y,z,\omega)$, $\Xi(x,y,\omega)$ and $\hat{\Xi}(x,y,\omega)$, respectively. For the spectrum of the phase shift of the beam of probing light $\varphi(x,y,t) - (4\pi/\lambda)n_0 L$, we use the notation $\Phi(x,y,\omega)$. The change to spectral amplitudes corresponds to a continuous mode of operation of the transducer. According to Eq. (2), the spectrum of the seeming displacement (i.e., the displacement that is obtained from the laser vibrometer readings without allowance for the effect of the medium) is expressed through the spectra of the true displacement and sound pressure as follows:

$$\hat{\Xi}(x,y,\omega) = n_0\Xi(x,y,\omega) - \gamma\int_0^L P(x,y,z,\omega)\,dz. \quad (4)$$

For spectral amplitudes, the wave equation transforms to the Helmholtz equation $\Delta P + (\omega^2/c^2)P = 0$. As is known, its solution can be represented by the angular spectral expansion

$$P(x,y,z,\omega) = \frac{1}{(2\pi)^2}\int_{-\infty}^{+\infty}\int_{-\infty}^{+\infty} dk_x dk_y$$

$$\times \Pi(k_x,k_y,\omega)e^{ik_x x + ik_y y + iz\sqrt{\frac{\omega^2}{c^2} - k_x^2 - k_y^2}}. \quad (5)$$

The latter expression takes into account the radiation condition: it only considers the waves propagating in the direction outward the radiating surface. In actual practice, this condition is violated as soon as acoustic waves reach the wall of the tank $z = L$, through which the beam of the probing laser is introduced, and begin to reflect from it. For simplicity, we assume that this wall perfectly absorbs acoustic waves. In this case, representation (5) proves to be valid. To determine the pressure of the spatial spectral amplitude $\Pi(k_x,k_y,\omega)$ (i.e., the angular spectrum), we expand the quantity $\Xi(x,y,\omega)$ into a spatial spectrum:

$$\Xi(x,y,\omega) = \frac{1}{(2\pi)^2}\int_{-\infty}^{+\infty}\int_{-\infty}^{+\infty} dk_x dk_y X(k_x,k_y,\omega)e^{ik_x x + ik_y y}. \quad (6)$$

According to the equation of motion, we have $\rho\,\partial^2\xi/\partial t^2 = -\partial p/\partial z|_{z=0}$. Substituting the full space–time expansions into this formula, we obtain the relationship between the pressure spectrum and the displacement spectrum: $\Pi(k_x,k_y,\omega) = -i\rho\omega^2 X(k_x,k_y,\omega)/\sqrt{\omega^2/c^2 - k_x^2 - k_y^2}$. Owing to the fact that, in the integrand in Eq. (5), the dependence on the z coordinate has a simple form, the integration along the beam presents no difficulties. Formula (4) yields the following expression for the spatial spectrum of the seeming displacement:

$$\hat{X}(k_x,k_y,\omega) = X(k_x,k_y,\omega)$$

$$\times \left[n_0 - \gamma\frac{\rho\omega^2\left(1 - e^{iL\sqrt{(\omega/c)^2 - k_x^2 - k_y^2}}\right)}{(\omega/c)^2 - k_x^2 - k_y^2} \right]. \quad (7)$$

Thus, we eliminated the sound pressure and obtained a direct relationship between the spectra of the true and seeming displacements. To determine the relationship between the initial functions $\xi(x,y,t)$ and $\hat{\xi}(x,y,t)$, it is necessary to apply the inverse Fourier transform.

If the liquid layer is sufficiently long ($L \to \infty$), the exponential $\exp\left(iL\sqrt{\omega^2/c^2 - k_x^2 - k_y^2}\right)$ can be ignored, because, in the presence of viscosity as small as one likes, this exponential will attenuate (the limiting

absorption principle). In practice, such a condition is not satisfied, because the dimensions of the tank containing the liquid are always small compared to the delay length of ultrasonic waves under study. However, the exponential can also be ignored in the case when the acoustic wave did not yet reach the edge of the liquid medium. The latter condition can be satisfied in the pulsed mode of transducer operation within a certain initial interval of time. Thus, in the two aforementioned cases, Eq. (7) takes the form

$$\hat{X}(k_x, k_y, \omega) = n_0 X(k_x, k_y, \omega) \frac{(\omega/c_*)^2 - k_x^2 - k_y^2}{(\omega/c)^2 - k_x^2 - k_y^2}. \quad (8)$$

Here,

$$c_* = \frac{c}{\sqrt{1 - \gamma \rho c^2/n_0}} = c\sqrt{n_0/n_*}. \quad (9)$$

According to Eq. (8), the role of the acousto-optic effect is reduced to spatial filtering of the spectrum of surface displacement. This result was earlier obtained in [13]. The filter is such that the spectral components corresponding to the condition $k_x^2 + k_y^2 = (\omega/c)^2$ are unboundedly amplified. This condition is nothing but the dispersion law for the displacement waves propagating along the surface of the transducer with the velocity of sound in the immersion medium (in the liquid). This explains why laser vibrometry used in the continuous mode of operation reveals a seeming inhomogeneity whose period coincides with the wavelength of ultrasound in the liquid (Fig. 2), whereas, in the pulsed mode of operation, the image exhibits regions that move with the velocity of sound in the liquid (Fig. 3).

We note that, by contrast, inhomogeneities with the dispersion law $k_x^2 + k_y^2 = \omega^2/c_*^2$ are completely suppressed. The corresponding disturbances have the form of waves propagating with the velocity $c_* > c$. This means that, if elastic waves with the velocity c_* propagate over the surface of the transducer, they will be invisible to the laser vibrometer. For water, the value of this velocity is $c_* \approx 1700$ m/s.

Spatial filtering (8) is equivalent to the following convolution:

$$\hat{\Xi}(x, y, \omega) = \iint dx' dy' \, \Xi(x', y', \omega)$$
$$\times K_\omega(x - x', y - y'), \quad (10)$$

where the kernel $K_\omega(x, y)$ is the Fourier transform of the spatial filter function. As one can see from Eq. (10), the kernel $K_\omega(x, y)$ represents the reading of the laser vibrometer $\hat{\Xi}$ that corresponds to the true displacement with the spectral amplitude $\Xi(x, y, \omega) = \delta(x)\delta(y)$, i.e., the displacement localized at the origin of coordinates. An explicit expression

for $K_\omega(x, y)$ can be most easily obtained from the Rayleigh integral without considering the angular spectrum. The Rayleigh integral has the form

$$P(x, y, z, \omega) = -\frac{\rho \omega^2}{2\pi} \iint dx' dy' \, \Xi(x', y', \omega) \frac{e^{i\frac{\omega}{c}R}}{R}, \text{ where}$$

$R = \sqrt{(x - x')^2 + (y - y')^2 + z^2}$. Substituting this expression for P into Eq. (4) and taking $L \to \infty$, we arrive at Eq. (10) in which

$$K_\omega(x, y) = n_0 \delta(x)\delta(y) + i \frac{\gamma \rho \omega^2}{4} H_0^{(1)}\left(\frac{\omega}{c}\sqrt{x^2 + y^2}\right). \quad (11)$$

Here, the Hankel function $H_0^{(1)} = J_0 + i Y_0$ corresponds to diverging waves.

Expression (10) with kernel (11) allows us to calculate the seeming displacement from the true surface displacement of the transducer in the case of its harmonic excitation. Knowing the displacement, by applying the Rayleigh integral, it is easy to calculate the generated acoustic field. The fact that the readings of the laser vibrometer may widely differ from the true displacement distribution on the surface of the transducer was mentioned above (see Fig. 4). It is of interest to analyze how this fact will influence the structure of the acoustic field. Figure 6 illustrates the corresponding characteristic features for the case of a circular plane transducer with a diameter of 30 mm, an operation frequency of 0.5 MHz and a uniform (piston-type) distribution of displacements. The thin line in the inset represents the aforementioned distribution Ξ. The thick line in the inset represents the distribution of visible displacement $\hat{\Xi}$ distorted by the acousto-optic effect. Within the source, vibrations arise with a period identical to the wavelength in the liquid (3 mm). Beyond the source, the quantity $\hat{\Xi}$ does not oscillate, but still has a considerable level of about 30% of the level at the transducer; it slowly decreases with an increasing transverse coordinate. The main plot shows the distribution of the amplitude of sound pressure along the symmetry axis of the source. The pressure is normalized by the quantity $P_0 = \rho c V_0$, where V_0 is the amplitude of the surface velocity of the piston-type transducer. The behavior of pressure for the piston-type source is shown by the thin line. The thick line represents the distribution that is obtained by calculating the pressure on the basis of the Rayleigh integral when the readings of the laser vibrometer are considered as true displacements. One can see that the true distribution does not coincide with the distribution calculated with the use of the vibrometer readings. In the far field, the curves differ only slightly, whereas, near the source, at a distance on the order of its diameter, they differ widely. Thus, the readings of the vibrometer cannot be directly used for transducer characterization.
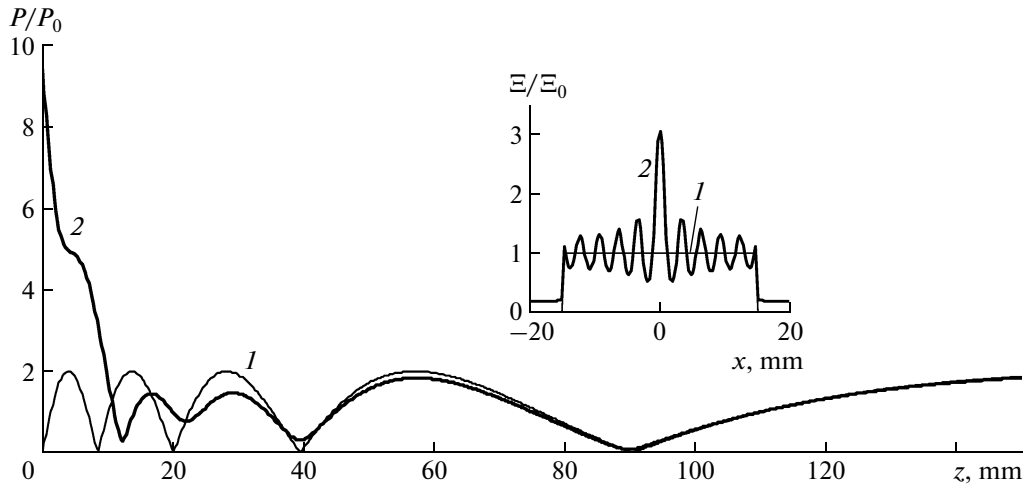
Fig. 6. The main plot represents the amplitude of normalized pressure versus the distance along the axis of a circular transducer. Curves *1* and *2* are calculated on the basis of the Rayleigh integral with the use of the distributions of the source surface displacements, Ξ and $\hat{\Xi}$, shown in the inset. The integration was performed over the transducer surface only. The inset shows (*1*) the normalized distribution of the true displacement amplitude Ξ and (*2*) the data of the laser vibrometer $\hat{\Xi}$ calculated from Eqs. (10) and (11).

It is worth noting that the function $K_\omega(x,y) - n_0\delta(x)\delta(y)$ proves to coincide with the Green's function for cylindrical waves. This is not surprising, because the correction $\varsigma(x,y,t) \equiv \hat{\xi} - n_0\xi$ is the solution to the inhomogeneous wave equation $\Delta_\perp\varsigma - c^{-2}\partial^2\varsigma/\partial t^2 = \gamma\rho\partial^2(\xi - \xi_L)/\partial t^2$, where $\Delta_\perp = \partial^2/\partial x^2 + \partial^2/\partial y^2$ and $\xi_L(x,y,t)$ is the z component of displacement of the liquid particle at a distance L from the source, i.e., under the assumption that the wall of the tank perfectly absorbs the wave incident on it. The above equation immediately follows from Eq. (7), if we multiply the latter by $\omega^2/c^2 - k_x^2 - k_y^2$ and apply the inverse Fourier transform with respect to coordinates and time. As long as the wave does not reach the wall of the tank, $\xi_L = 0$, the following equation is valid for the displacement ς:

$$\Delta_\perp\varsigma - \frac{1}{c^2}\frac{\partial^2\varsigma}{\partial t^2} = \gamma\rho\frac{\partial^2\xi}{\partial t^2}. \tag{12}$$

Let us consider several solutions to Eq. (12), which illustrate the effect of acousto-optic interaction on the readings of the laser vibrometer. Let, for example, a plane elastic wave $\xi = \xi_0(x - Vt)$ propagate over the surface under study with velocity V. If we consider a steady-state process, the solution to Eq. (12) should be sought in the form $\varsigma = \varsigma_0(x - Vt)$. After substitution and integration, we obtain $\varsigma_0(x) = \gamma\rho V^2(1 - V^2/c^2)^{-1}\xi_0(x)$, i.e., $\hat{\xi} = \left[n_0 + \gamma\rho V^2(1 - V^2/c^2)^{-1}\right]\xi$. From this expression, one can see that the signal of the laser vibrometer adequately indicates the profile of the surface displacement. However, the magnitude of the visible displacement $\hat{\xi}$ depends on the velocity of the surface wave and may considerably differ from the true displacement ξ. In particular, at low velocities $\hat{\xi} \approx n_0\xi$ at $V \to c$, the signal unboundedly increases and at $V \gg c$, the signal proves to be identical to that in the piston-type source: $\hat{\xi} \to (n_0 - \gamma\rho c^2)\xi$.

Let us consider another case, which concerns the readings of the laser vibrometer near the edge of the transducer under pulsed excitation. Let at $t = 0$ the half-plane $x > 0$ be displaced in a jumplike manner by $\Delta\xi$; i.e., the initial condition has the form $\xi(x,y,t = 0) = \Delta\xi\Theta(x)$, where $\Theta(x)$ is the Heaviside step function. The quantity ξ, which is the solution to the wave equation $\Delta_\perp\xi - V^{-2}\partial^2\xi/\partial t^2 = 0$, for $t > 0$ is described by the expression $\xi = (\Delta\xi/2) \times [\Theta(x - Vt) + \Theta(x + Vt)]$. Substituting this expression into the right-hand side of Eq. (12) and taking into account that $\varsigma(x,t = 0) = 0$, we obtain the following formula for the visible displacement:

$$\begin{aligned}
\hat{\xi} = \frac{\Delta\xi}{2}\Theta(t)\Bigg\{ &\left(n_0 - \frac{\gamma\rho V^2}{(V/c)^2 - 1}\right) \\
&\times[\Theta(x - Vt) + \Theta(x + Vt)] \\
&+ \frac{\gamma\rho V^2}{(V/c)^2 - 1}[\Theta(x - ct) + \Theta(x + ct)]\Bigg\}.
\end{aligned} \tag{13}$$

From this formula, it follows that the readings of the laser vibrometer contain both the true wave and the artifact wave caused by acousto-optic interaction. According to Eq. (13), the amplitude ratio of the corresponding signals is $(c^{-2} - c_*^{-2})/(V^{-2} - c_*^{-2})$. In partic-

ular, when $V \to c_*$, it tends to infinity, because the image of the corresponding true wave disappears. Note that the artifact waves propagating with velocity c are truly observed in the experiment: for example, in Fig. 3, one can see clearly defined waves possessing a linear front and diverging from the edges of the square transducer.

3.3. Distortion of the Signal in the Transient Mode of Operation

When analyzing the signal of the vibrometer in the transient mode of operation, one should know the type of signal shown by the vibrometer in the case of a displacement of a pulsed point: $\xi = \delta(x)\delta(y)\delta(t)$. The corresponding pulsed response $\hat{\xi} = H(x,y,t)$ can be used to calculate the signal of the vibrometer in the case of an arbitrary displacement distribution over the source surface. In Eq. (11), the kernel is the spectrum of the pulsed response $H(x,y,t)$. Applying the inverse Fourier transform, we obtain

$$H(x,y,t) = n_0 \delta(x)\delta(y)\delta(t)$$
$$-\frac{\gamma\rho}{2\pi}\frac{\partial^2}{\partial t^2}\left[\frac{\Theta\left(t - \sqrt{x^2+y^2}/c\right)}{\sqrt{t^2 - (x^2+y^2)/c^2}}\right]. \qquad (14)$$

The general relation between the true and seeming displacements has the form of a three-dimensional convolution:

$$\hat{\xi}(x,y,t) = n_0 \xi(x,y,t)$$
$$-\frac{\gamma\rho}{2\pi}\int_{-\infty}^{\infty}\int_{-\infty}^{\infty} dx'dy'\int_{-\infty}^{t-\frac{r}{c}}\frac{w(x',y',t')dt'}{\sqrt{(t-t')^2 - r^2/c^2}}. \qquad (15)$$

Here, $w(x,y,t) = \partial^2\xi/\partial t^2$ is the acceleration of surface points. In addition, to make the formula shorter, we introduced the notation $r = \sqrt{(x-x')^2 + (y-y')^2}$. Using Eq. (15), we consider the practically important case of the signal of the laser vibrometer under the conditions where the transducer, being initially turned off, is turned on at a certain instant (say, $t = 0$) and begins vibrating according to the sinusoidal law. As will be seen below, the signal of the vibrometer becomes steady-state only after a while, and this does not always happen before the acoustic wave reaches the wall of the tank, through which the probing laser beam is introduced ($z = L$). Since, after the reflection of the acoustic wave from the wall, the acousto-optic interaction process becomes rather complicated, one may expect that experimental implementation of a continuous mode of operation in tanks of relatively small size is impossible. Below, we show that this assumption fails.

When the sinusoidal signal $\xi(x,y,t) = A(x,y)\,e^{-i\omega t}\Theta(t)$ is turned on, the surface acceleration at $t > 0$ has the form $w(x,y,t) = -\omega^2 A(x,y)e^{-i\omega t}$. From Eq. (15), after some transformations, we obtain

$$\hat{\xi}(x,y,t) = n_0 \xi(x,y,t)$$
$$+\frac{\gamma\rho\omega^2}{2\pi}e^{-i\omega t}\int_{-\infty}^{+\infty}\int_{-\infty}^{+\infty} dx'dy'\, A(x',y')\Theta\left(t - \frac{r}{c}\right)$$
$$\times\left\{\int_{r/c}^{\infty}d\tau\frac{e^{i\omega\tau}}{\sqrt{\tau^2 - r^2/c^2}} - \int_{t}^{\infty}d\tau\frac{e^{i\omega\tau}}{\sqrt{\tau^2 - r^2/c^2}}\right\}.$$

The first inner integral is a tabular one: $\int_{r/c}^{\infty}d\tau\frac{e^{i\omega\tau}}{\sqrt{\tau^2 - r^2/c^2}} = i\frac{\pi}{2}H_0^{(1)}\left(\frac{\omega}{c}r\right)$. We are interested in a quasi-stationary envelope. Such a mode of operation is reached when $t \gg r_{max}/c$, where r_{max} is the distance from the point of observation to the most distant point of the transducer surface. Under this condition, we have

$$\int_{t}^{\infty}d\tau\frac{e^{i\omega\tau}}{\sqrt{\tau^2 - r^2/c^2}} \approx \int_{t}^{\infty}d\tau\frac{e^{i\omega\tau}}{\tau}$$
$$= -[\text{ci}(\omega\tau) + i\text{si}(\omega\tau)] \approx i\frac{e^{i\omega t}}{\omega t}.$$

As a result, we obtain

$$\hat{\xi}(x,y,t) = n_0 \xi(x,y,t)$$
$$+i\frac{\gamma\rho\omega^2}{4}\int_{-\infty}^{+\infty}\int_{-\infty}^{+\infty} dx'dy'\, A(x',y')e^{-i\omega t}H_0^{(1)}\left(\frac{\omega}{c}r\right)$$
$$-i\frac{\gamma\rho\omega}{2\pi t}\int_{-\infty}^{+\infty}\int_{-\infty}^{+\infty} dx'dy'\, A(x',y').$$

Using the fact that, within the time interval under consideration, we have $A(x,y)\,e^{-i\omega t} = \xi(x,y,t)$ and taking into account Eq. (11), we arrive at the conclusion that the first two terms give exactly the same result as that obtained earlier for the steady-state mode of operation. Hence, the last term characterizes the transient process. It is important that this term slowly varies within the scale on the order of the wave period ($\sim t^{-1}$) and does not depend on the coordinates of the observation point (x,y). Therefore, it weakly affects the phase of the wave and its amplitude, if the latter is measured as half the peak-to-peak amplitude of the signal, or the signal is preliminarily passed through a high-frequency filter. Hence, at finite times satisfying the condition $r_{max}/c \ll t < L/c$, the characteristics of the steady-state signal can be measured with the use of tanks of relatively small size L.

3.4. Compensation of Distortions Caused by Acousto-Optic Interaction (The Inverse Problem)

Let us invert relation (8) between the spectra of the true and seeming displacements:

$$X(k_x, k_y, \omega) = \frac{\hat{X}(k_x, k_y, \omega)}{n_0} \frac{(\omega/c)^2 - k_x^2 - k_y^2}{(\omega/c_*)^2 - k_x^2 - k_y^2}. \quad (16)$$

Thus, if we perform the aforementioned correction of the angular spectrum, we can compensate the effect of acousto-optic interaction in the absence of noise. Here, the main difficulty is that the function of such a filter contains a singularity at $k_x^2 + k_y^2 = \omega^2/c_*^2$. This leads to an infinite amplification of the corresponding noise, i.e., makes the correction process impossible. To avoid the undesired amplification of noise, we can artificially eliminate the singularity in Eq. (16). However, we will not discuss such regularization in this paper.

There is one more fundamental difficulty in the implementation of the algorithm proposed above for compensation of the acousto-optic effect. For calculating the spatial spectrum $\hat{X}(k_x, k_y, \omega)$, it is necessary to know the corresponding seeming displacement $\hat{\Xi}(x, y, \omega)$ throughout the entire (x, y) plane, rather than within the source boundaries. From the example shown in the inset in Fig. 6, one can see that the quantity $\hat{\Xi}$ remains significant far beyond the source boundaries. In other words, the probing beam of the vibrometer should scan not only over the surface of the source itself, but also over a large area around the source. However, such a measurement may be impossible in practice, because an actual transducer always has a finite size while, beyond its boundaries, the probing beam encounters no surface to be reflected from. Thus, to provide the fundamental possibility for solving the inverse problem, it is necessary to use tanks whose size far exceeds the diameter of the source and also to place a wide-aperture reflecting screen beyond the source boundaries.

Solution of the inverse problem can be reduced to solving an auxiliary direct problem on the basis of using the inhomogeneous wave equation that follows from Eq. (16):

$$\Delta_\perp \xi - \frac{1}{c_*^2} \frac{\partial^2 \xi}{\partial t^2} = \frac{1}{n_0} \left(\Delta_\perp \hat{\xi} - \frac{1}{c^2} \frac{\partial^2 \hat{\xi}}{\partial t^2} \right). \quad (17)$$

In the pulsed mode of excitation, within a certain initial time interval, Eq. (17) allows us to avoid the aforementioned difficulties arising in the compensation of the acousto-optic effect (above, these difficulties were discussed in application to the continuous excitation mode). The right-hand side of Eq. (17) is known if the visible displacement $\hat{\xi}(x, y, t)$ is measured. Note that, if $\hat{\xi}$ contains signals in the form of waves propagating with velocity c, they will make no contribution to the right-hand side, i.e., will not manifest themselves. In contrast, if $\hat{\xi}$ contains disturbances propagating with velocity c_*, these signals will be resonant and the corresponding component of the reconstructed displacement ξ will be significant. As was noted above, the characteristic feature of acousto-optic interaction consists in that no such signals should be present in the distribution of $\hat{\xi}$. However, in an actual experiment, they necessarily arise because of the presence of noise, which already was noted above.

CONCLUSIONS

Laser vibrometry has been used for years in various fields of science and engineering and is believed to be a precise method of measuring absolute surface displacements [2, 10, 14]. The latter is true when the vibrating surface under investigation is in air (or in some other gas). In this paper, we showed that, when measurements are performed in a liquid, the data obtained from a laser vibrometer for the point of incidence of the probing laser beam is erroneous, and the deviation of the visible displacement from the true one may exceed the true displacement itself. Moreover, not only do the absolute values of displacements at individual points, but also the form of the distribution of two-dimensional displacement over the surface under study differ from the true ones. In particular, the visible vibration pattern contains a false structure with a spatial scale identical to the wavelength of acoustic waves in the liquid. In addition, the laser vibrometer indicates displacements in the regions where they are actually absent. In the transient mode of operation, the image displays nonexisting surface waves propagating with the velocity of sound in the liquid. The origin of these distortions lies in the acousto-optic interaction that occurs in the condensed medium on the path of the probing laser beam.

The aforementioned features of laser vibrometry that were observed in our experiments were theoretically analyzed. In addition to the well-known analysis of acousto-optic interaction by introduction of an equivalent spatial filter, we derived an analytical expression for the function characterizing the acousto-optic response to a local surface displacement $\xi \sim \delta(x)\delta(y)$ under harmonic excitation and the corresponding function of the pulse response, i.e., the acousto-optic addition in the case of displacement of the form $\xi = \delta(x)\delta(y)\delta(t)$. Different versions of the solution were analyzed and it was shown that the solution explains all the artifacts of laser vibrometry in liquid that were observed in our experiments.

The process of the establishment of the vibrometer signal after the beginning of harmonic excitation of an initially nonexcited transducer was theoretically investigated. It was shown that steady-state values of signal amplitude and phase can be correctly measured well

before the signal reaches its steady-state level when the measurements are performed within time intervals on the order of several travel times of sound within the source size. In a laboratory experiment, this allows one to avoid interference caused by multiple reflections of acoustic waves in the measuring tank containing the liquid. The measurement of two-dimensional distributions of steady-state amplitude and phase values throughout the source surface makes it possible to apply the inverse filtering algorithm and to reconstruct the true surface displacement within certain approximation. Such a reconstruction is impossible for disturbances in the form of surface waves propagating with the velocity of sound in the liquid.

ACKNOWLEDGMENTS

REFERENCES

1. N. A. Halliwell, *Laser Vibrometry Optical Methods in Engineering Metrology,* Ed. by D. C. Williams (Chapman and Hall, London, 1993), ch. 6, pp. 179–211.

2. P. Gendreu, M. Fink, and D. Royer, IEEE Trans. Ultrason., Ferroelect. Freq. Control **42**, 135 (1995).

3. D. Cathignol, O. A. Sapozhnikov, and J. Zhang, J. Acoust. Soc. Am. **101**, 1286 (1997).

4. W. A. Smith and B. A. Auld, IEEE Trans. Ultrason. Ferroelec. Freq. Control **38**, 40 (1991).

5. D. Cathignol, O. A. Sapozhnikov, and Y. Theillere, J. Acoust. Soc. Am. **105**, 2612 (1999).

6. J.-Y. Chapelon, D. Cathignol, C. Cain, et al., Ultrasound Medicine Biol. **26**, 153 (2000).

7. C. V. Raman and K. S. Venkataraman, Proc. R. Soc. London, Ser. A **171**, 137 (1939).

8. D. R. Bacon, R. C. Chivers, and J. N. Som, Ultrasonics **31** (5), 321 (1993).

9. O. A. Sapozhnikov, A. V. Morozov, and D. Cathignol, in *Proc. of the IEEE UFFC 50th Ann. Joint Conf., Montreal, Canada, Aug. 23–27, 2004,* pp. 161–164.

10. D. R. Bacon, IEEE Trans. Ultrason., Ferroelect. Freq. Control **35**, 152 (1988).

11. D. Royer, N. Dubois, and P. Benoist, in *IEEE Ultrason. Symp. Proc.* (1992), p. 805.

12. C. Koch and W. Molkenstruck, IEEE Trans. Ultrason., Ferroelect. Freq. Control **46**, 1303 (1999).

13. D. Certon, Matar O. Bou, J. Guyonvarch, et al., in *IEEE Ultrason. Symp. Proc.* (2001), p. 1065.

14. Yu. V. Zhitlukhina, D. V. Perov, and A. B. Rinkevich, Akust. Zh. **54**, 110 (2008) [Acoust. Phys. **54**, 94 (2008)].

Translated by E. Golyamina